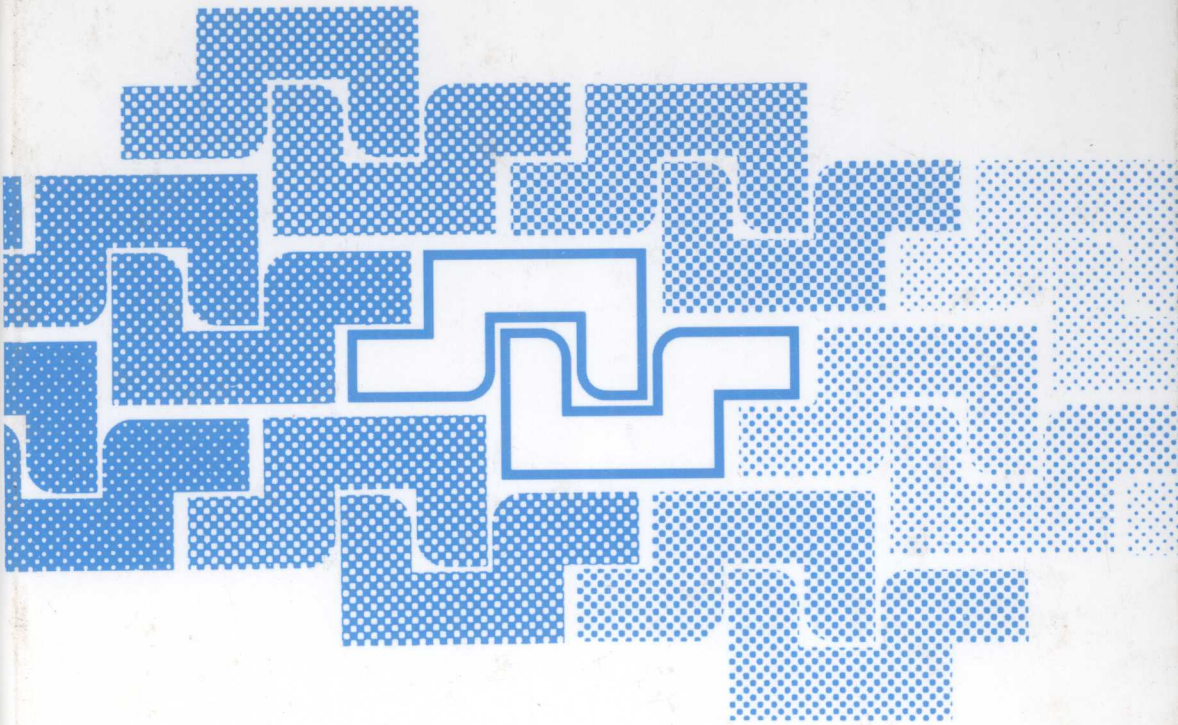

Molecular Nanowires and Other Quantum Objects

Edited by

Alexandre S. Alexandrov, Jure Demsar
and Igor K. Yanson

NATO Science Series

Molecular Nanov  er
Quantum Objects

edited by

Alexandre S. Alexandrov

Loughborough University,
Physics Department,
Loughborough, United Kingdom

Jure Demsar

"Jozef Stefan" Institute,
Ljubljana, Slovenia

and

Igor K. Yanson

B. Verkin Institute for Low Temperature Physics and Engineering,
National Academy of Sciences of Ukraine,
Kharkiev, Ukraine

Kluwer Academic Publishers

Dordrecht / Boston / London

Published in cooperation with NATO Scientific Affairs Division

Proceedings of the NATO Advanced Research Workshop on
Molecular Nanowires and Other Quantum Objects
Bled, Slovenia
7–9 September 2003

A C.I.P. Catalogue record for this book is available from the Library of Congress.

ISBN 1-4020-2068-6
ISBN 1-4020-2093-7 (e-book)

Published by Kluwer Academic Publishers,
P.O. Box 17, 3300 AA Dordrecht, The Netherlands.

Sold and distributed in North, Central and South America
by Kluwer Academic Publishers,
101 Philip Drive, Norwell, MA 02061, U.S.A.

In all other countries, sold and distributed
by Kluwer Academic Publishers,
P.O. Box 322, 3300 AH Dordrecht, The Netherlands.

Printed on acid-free paper

PREFACE

There is a growing understanding that the progress of the conventional silicon technology will reach its physical, engineering and economic limits in near future. This fact, however, does not mean that progress in computing will slow down. What will take us beyond the silicon era are new nano-technologies that are being pursued in university and corporate laboratories around the world. In particular, molecular switching devices and systems that will self-assemble through molecular recognition are being designed and studied. Many laboratories are now testing new types of these and other reversible switches, as well as fabricating nanowires needed to connect circuit elements together. But there are still significant opportunities and demand for invention and discovery before nanoelectronics will become a reality. The actual mechanisms of transport through molecular quantum dots and nanowires are of the highest current experimental and theoretical interest. In particular, there is growing evidence that both electron-vibron interactions and electron-electron correlations are important. Further progress requires worldwide efforts of trans-disciplinary teams of physicists, quantum chemists, material and computer scientists, and engineers.

The NATO Advanced Research Workshop "Molecular Nanowires and Other Quantum Objects" brought together 40 experts in molecular and other nanowires, carbon nanotubes, mesoscopic superconductors and semiconductors, and theorists in the field of strongly correlated electrons and phonons from 14 NATO, NATO-Partner and Mediterranean-Dialogue countries working in 32 university and corporate laboratories. Topics for discussion included molecular nanojunctions and electronics, mesoscale semiconductors and superconductors, carbon nanotubes, low dimensional conductors, polarons and strongly-correlated electrons in nanoobjects, quantum theory of nanoscale, including first-principle simulations, new techniques for making mesoscopic sensors and detectors. The framework of the meeting allowed participants to become acquainted with a diverse cross-spectrum of available skills, and to engage in exchanging their often-complementary experiences and views. Many participants acknowledged the program as very stimulating and well-organised. These resulting proceedings of the NATO ARW on 'Molecular Nanowires and Other Quantum Objects' represent a tiny but important part of the activities in the field.

It is our pleasant duty to acknowledge the wide assistance we received. We greatly appreciate the Science Programme of NATO in Brussels for funding the Workshop. In addition, the members of the organizing committee Alexander F. Andreev, Viktor V. Kabanov and R. Stanley Williams deserve special thanks for their efforts in organizing the final program. Furthermore, we would like to acknowledge Dragan Mihailovic and Nika Simcic (Quantum Materials Group at Jozef Stefan Institute) for their support and help before and during the workshop. Finally, we would like to thank R. Stanley Williams (Hewlett Packard Labs) for letting us use the photo of the HP 64-bit molecular memory as the conference logo.

Sasha Alexandrov
Jure Demsar
Igor Yanson

December, 2003

TABLE OF CONTENTS

CARBON NANOTUBES

SUPERCONDUCTING NANOSTRUCTURES

POLARONS

COMPLEX QUANTUM DOTS

NANOSTRUCTURES

MESOSCOPIC SUPERCONDUCTORS

SPIN-POLARIZED NANOOBJECTS

FUNDAMENTALS OF NANOSCALE

LOW DIMENSIONAL QUANTUM OBJECTS

CHARACTERIZATION OF NANOSCALE MOLECULAR JUNCTIONS

Artur Erbe, Zhenan Bao, David Abusch-Magder, Donald M. Tennant, and Nikolai Zhitenev

Lucent Technologies, Bell Labs, 600 Mountain Avenue, Murray Hill, NJ, 07974, USA

aerbe@lucent.com

Abstract Two methods for formation of metal-molecule-metal junctions are demonstrated. The use of different techniques allows us to contact short molecules approaching the single molecule limit as well as longer polymers in single layers. The sample geometries also enable us to test gate dependencies on some of the tested structures.

Keywords: Nanoscale Molecular Junctions, metal-molecule-metal junctions

1. Introduction

Exploring the electronic possibilities of nanoscale organic materials has become an important challenge as modern lithographical techniques approach ultimate limits. In this regime, the properties of single or few molecules can dominate the behavior of whole devices. Recent experiments on nanoscale molecular junctions show a large variety of results [1, 2, 3, 4, 5]. Values of the conductivity as well as energy scales of the states participating in current transport vary over a broad range. Differences in the properties of the molecules themselves can only explain some of these variations. This fact indicates that details of the contact formation to the molecules play an important role in the behavior of the whole junction and control of the contact properties is a highly important prerequisite for successful testing of molecular behavior on this scale. We present electrical measurements of various types of molecules using two recently developed contacting techniques. Both methods allow us to contact single or a few molecules electrically and characterize them under varying conditions. The first technique is based on shadow stencil mask evaporation similar to the well-known metallic Single Electron Transistor (SET) fabrication [6]. The mask is defined by electron beam lithography (EBL) in direct contact with the substrate. The second technique presented here uses two closely spaced electrodes defined by EBL that are covered by the molecules.

A.S. Alexandrov et al. (eds.), Molecular Nanowires and Other Quantum Objects, 1–12.

Electrical characterization is done on molecules bridging the distance between the electrodes. This method is especially useful for characterization of longer polymers. We performed measurements on a variety of molecules using both techniques. Distinct features are found in the I-V-characteristics at low temperatures indicating that single or a few molecules are contacted. Some of those features can be affected by changes in applied gate voltage.

2. Fabrication

The measurements reported in this paper were performed on "short" (three rings of phenyl or thiophene in series) molecules and "long" (Poly-thiophene and Poly-fluorene) polymers. Two different techniques have to be developed in order to reliably connect to both kinds of molecules. In case of the short molecules we can rely on the formation of a Self Assembled Monolayer (SAM) on a gold surface in order to separate the two contacting gold electrodes. Therefore a shadow evaporation technique can be used to contact these molecules. The long polymers do not form a well ordered monolayer. Thus they are contacted by two EBL defined electrodes separated by a very small distance.

The lengthscales of short single molecules (1 to 2 nm) are not accessible by traditional fabrication techniques. Furthermore the SAM is destroyed if the structures are processed with standard lithography after deposition of the molecules. Using a shadow stencil mask for the definition of the contacts we avoid exposure of the SAM to any harmful chemistry.

Shadow masks based on resist bilayers (PMMA/MMA, for example) have been used for the fabrication of nanoscale structures like metallic SETs for a long time [6]. The double layer resist is attacked by the solvents of the molecules (usually THF (TetraHydroFuran) in case of our molecules) and can be destroyed during self assembly of the monolayer or contaminate the SAM. We therefore choose a combination of SiO_2 and Si_3N_4 as mask material. This double layer is structured using EBL. The pattern of the mask is transferred to the double layer using two consecutive dry-etch steps. A detailed description of the fabrication process is shown in figure 1.

After the definition of the mask gold contacts are evaporated perpendicular to the sample surface. This creates two gold fingers on the left- and right-hand side of the SiO_2 -bridge separated by 50-100 nm. In order to form a SAM on the gold, the sample is soaked in a molecular solution for several hours. A second evaporation step is performed on the tilted sample in order to connect both contacts through the monolayer under the bridge (a schematic drawing is shown in figure 2).

The tilting angle of the sample determines the overlap between the upper and lower gold and thus the area of the junction. Monitoring the conductivity between source and drain during this second evaporation step and changing

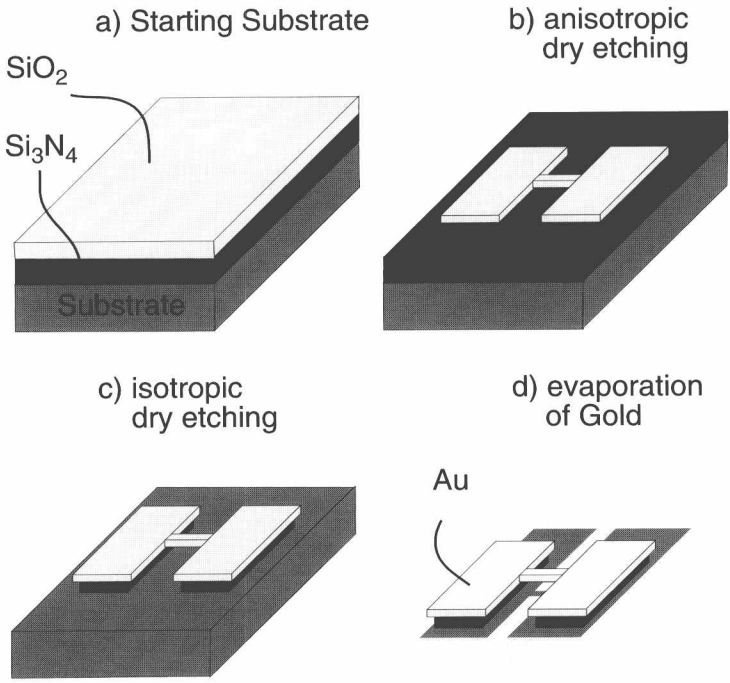

Figure 1. Fabrication of a shadow mask with smallest dimensions around 100 nm. **a)** The substrate is covered with PECVD deposited Si_3N_4 (200 nm) and SiO_2 (100 nm). **b)** Definition of the shadow mask using EBL. The resist serving as a mask for the etch steps is PMMA. The transfer into the SiO_2 -layer is done by anisotropic reactive ion etching (etch gas CHF_3). **c)** Isotropic reactive ion etching (etch gas CF_4) removes the Si_3N_4 under and around the places where the SiO_2 layer was opened. A small bridge (50-100 nm wide) is left in the center of the structure. **d)** Definition of the metallic contacts by vertical evaporation of gold.

the tilting angle can ensure that the evaporation is stopped at the first onset of conductance and thus single or only a few molecules are contacted. A tantalum gate electrode (width 5μm) is defined in the center of the structure and covered by a gate oxide (50 nm of SiO_2) before the fabrication of the mask. A micrograph of the resulting structure can be seen in figure 3.

This method was used for molecules P3 and T3 (the molecules are shown in figure 4).

Thiol endgroups provide attachment to gold for self assembly and ensure good mechanical and electrical bond to the top gold contact. The central ring in the P3 molecule is rotated by about 45° around the backbone of the molecule. It is expected that this leads to differences in conductance behavior compared to T3, which is mostly flat [7]. Both molecules are completely conjugated, so a rather high conductance along the molecule is expected.

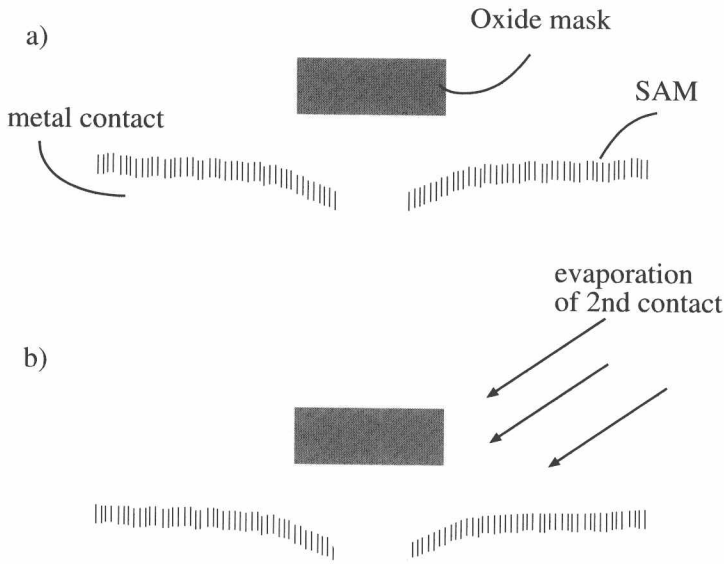

Figure 2. Evaporation on the shadow mask under different angles in order to produce nanoscale junctions **a)** Contacts are evaporated vertically through the shadow mask. A SAM is formed on both contacts. **b)** Evaporation on the tilted sample results in a connection between the two contacts through the monolayer. During this step the conductance of the junction can be monitored in order to ensure that contact is made to single or few molecules. The tilting angle and thus the overlap between top and bottom electrode can be changed during the second evaporation step.

In order to contact the polymers (length distribution centered around 50 nm) metal electrodes (15-20 nm of $Au_{0.6}Pd_{0.4}$) are defined by EBL with distances ranging from 5 to 20 nm. Typical structures are shown in figure 5.

The gate electrode in this setup is given by the substrate (highly doped Si) which is insulated by 90 nm of thermally grown SiO_2 .

3. Results

The measurements were performed in a low temperature probe station allowing for easy simultaneous access to many junctions. Thus we were able to measure a large amount of working samples although the yield of the production technique was still rather low. The main failure mechanism in the shadow mask technique results from shorts between the contacts and the gold layer on top of the mask. Three typical examples for the behavior of the remaining junctions at 4.2 K are given in the following discussion.

One group of curves strongly resembles Coulomb blockade behavior (shown in figure 6). These curves show a conduction gap around V_{sd}=0. The width of the gap ($\pm$100 mV) corresponds to Coulomb blockade on a metallic cluster

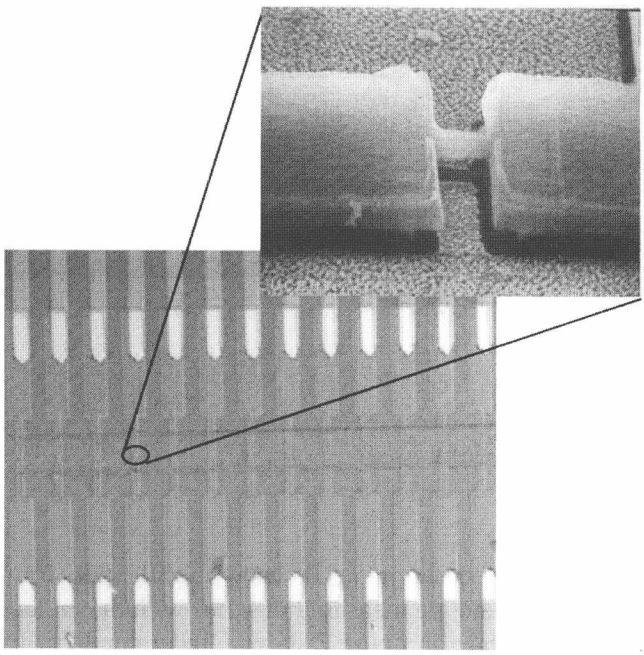

Figure 3. Micrograph of several shadow mask junctions produced in parallel. On the top and bottom the connecting pads leading to the small structures in the center can be seen. The mask material is covering these leads over most of the sample area in order to minimize shorts between the leads and the top gold-layer. Only the areas where EBL and optical lithography overlap make the connection between the big pads and the nanoscale electrodes. The gate electrode lies underneath the center part of the junctions (dark region in the center of the picture). Upper right: SEM micrograph of the central part of the mask after vertical evaporation of gold.

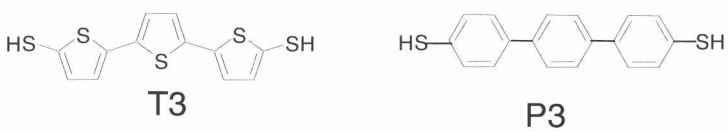

Figure 4. Characterized molecules: T3 consists out of 3 thiophene rings, P3 out of 3 phenyl rings. Both molecules are designed with thiol endgroups on both ends

of 4–6 nm diameter. Similar curves are measured when small metal clusters are deposited on purpose on top of the SAM before the second evaporation step (This measurement was done in the geometry discussed in [8]). It is

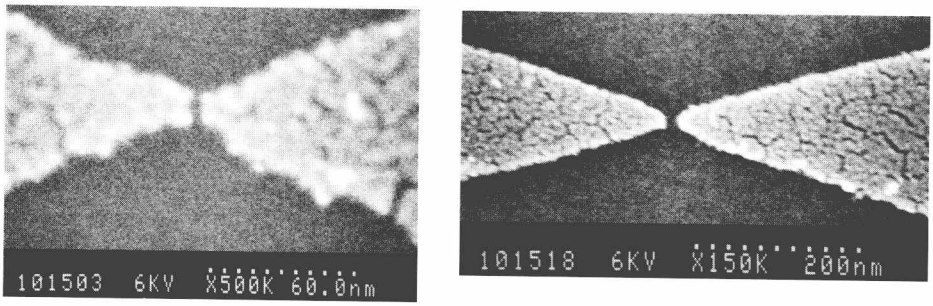

Figure 5. SEM-micrograph of two EBL defined contacts with gaps of few nanometers.

therefore likely that in this situation metal clusters accidentally form during the second evaporation step and are measured in series with the molecules.

The measurements shown in figure 7 show a lower conductivity. This can indicate that the area of the measured junction is reduced compared to junctions characterized in figure 6.

The I-V-curves exhibit a series of clear periodic steps. The energy scale for these steps is smaller than the energy scale calculated from the gap in figure 6 by a factor of 2–3. Some of these measurements show also a non zero conductivity at zero bias. Energy scales extracted from temperature dependence reveal an even lower energy scale, in the range of a few meV, similar to the energy scale obtained from larger junctions (see below). Hence the behavior differs from the Coulomb blockade behavior on small clusters and the properties have to be attributed to a different mechanism. The distance between consecutive steps depends on the chosen molecule. In figure 7 b) a measurement on T3 is shown for comparison. The period of the steps is about 100 mV in the case of T3, while it is about 50 mV in the case of P3. The overall conductance is comparable and very low. Qualitatively samples measured in a quartz fiber geometry on the same molecules show a very similar behavior [8]. On the other hand there are some obvious differences in the quantitative behavior. The most remarkable difference is the overall resistance. In the shadow mask geometry overall resistance of a single junction (estimated from the linear background) is around 100 GΩ, while typical resistance in the tip geometry is about 200 MΩ. The second quantitative difference is the spacing of the steps which is 22–50 mV for the T3 molecule in the quartz tip geometry. Both differences possibly result from the different coupling of the molecules to the electrodes in the two geometries. It can be seen in figure 3 that the bottom gold underneath

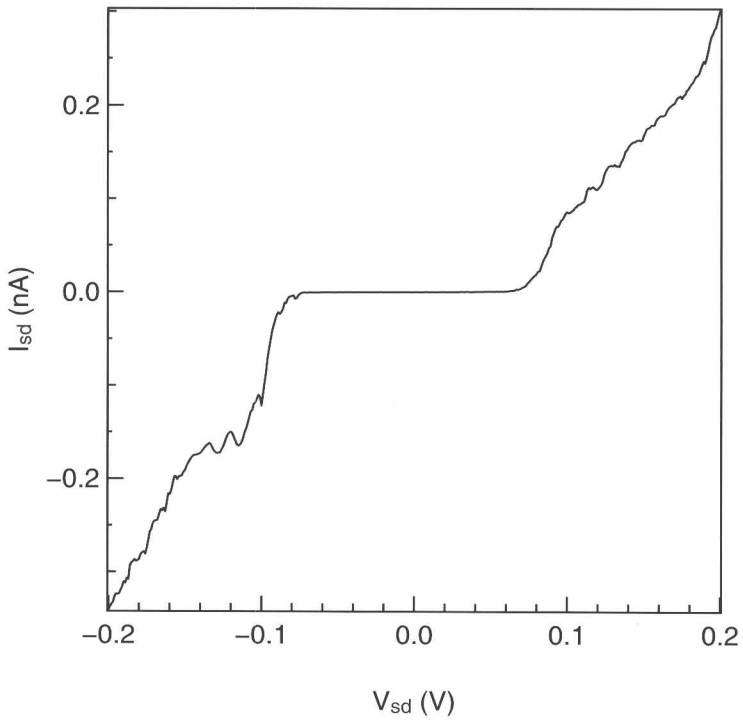

Figure 6. I-V-curve obtained from the shadow mask technique on P3 at 4.2 K. A conductivity gap extends from $V_{\mathrm{sd}} = -0.1$ V to $V_{\mathrm{sd}} = 0.1$ V. No further conductivity steps can be seen.

the shadow mask is rough due to the processing steps performed on the SiO_2 before evaporation of the gold. The coupling to the top electrode is probably weakened due to this roughness. This results in a reduced conductivity and can also explain the different energy scale of the resonances. One possible explanation for the resonances is tunneling through some low-energy states in the monolayer due to interaction between molecules and the metal. The features may also be explained by coupling of electronic states to molecular vibrations [8]. The energy scale for both mechanisms changes if the coupling to the metal changes. In case of molecular vibrations the mechanical boundary conditions change as well as the coupling of the different modes to the contacts. The tunneling through the low energy states depends on the height of the barrier between metal and molecules and thus also on the coupling.

In figure 7 a) we also present the gate dependence of one of the planar junctions. Some of the resonances react in a linear way to the applied gate voltage (as indicated by the arrow), some others react in less regular way. This result also resembles the behavior found in [8] qualitatively. Only a few

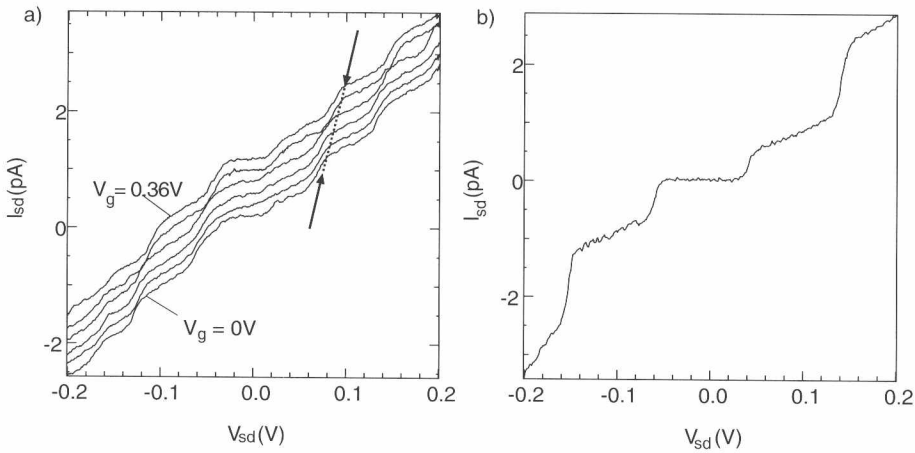

Figure 7. **a)** Measurement of P3 at 4.2 K. Strong resonances in the I-V-characteristics show that single or a few molecules are contacted. Measurements with applied gate voltage are offset vertically for clarity. **b)** Measurement of T3 at 4.2 K. Different periodicity of the steps is found compared to the measurements on P3.

samples show this clear gate dependence, while in most samples no gate effect is present. This behavior can also be explained by the strong surface roughness of the gold in the planar junction. In this situation contact formation to a molecule deposited on the top of the bottom electrode is much more likely than connecting a molecule on the sidewalls. Molecules on the top are electrostatically screened from the gate underneath the bottom electrode and do not show gate dependence.

In figure 8 a very smooth nonlinear curve is shown. Only a small suppression of conductivity around $V_{\mathrm{sd}} = 0$ can be seen, all other nonlinearities seen are averaged out. The overall conductance is larger than in figures 6 and 7. It is therefore likely that a larger area is probed in this measurement.

If the tilting angle during second evaporation is too large or the top metal is too thick too many molecules may bind to the top layer and contribute to the conduction. This can explain a smooth nonlinearity as seen in the measurement. The energy scale attributed to the suppression of conduction close to $V_{\mathrm{sd}} = 0$ is of the order of few meV. A similar energy scale is extracted from the temperature dependence.

Measurements on EBL-fabricated junctions were done on Poly-thiophene and Poly-fluorene (the length of both polymers is about 50 nm). The polymers are designed with thiol endgroups on both ends. Therefore some of the polymers will bind to both electrodes with one end on each electrode if the inter-electrode distance is below 50 nm. For preparation of the polymer film a